Crystalline Solids with Intrinsically Low Lattice Thermal Conductivity for Thermoelectric Energy Conversion

Article *in* ACS Energy Letters · May 2018

DOI: 10.1021/acsenergylett.8b00435

CITATIONS
110

READS
162

2 authors:

Manoj Kumar Jana
Duke University
28 PUBLICATIONS **1,040** CITATIONS
SEE PROFILE

Kanishka Biswas
Jawaharlal Nehru Centre for Advanced Scientific Research
191 PUBLICATIONS **13,814** CITATIONS
SEE PROFILE

ACS Energy LETTERS

Cite This: ACS Energy Lett. 2018, 3, 1315−1324

PERSPECTIVE

Crystalline Solids with Intrinsically Low Lattice Thermal Conductivity for Thermoelectric Energy Conversion

Manoj K. Jana and Kanishka Biswas*

New Chemistry Unit, Jawaharlal Nehru Centre for Advanced Scientific Research (JNCASR), Bangalore, India 560064

ABSTRACT: The extrinsic routes to manipulating phonon transport, for instance, through multiple defects of hierarchical length scales, are proven effective in suppressing the lattice thermal conductivity (κ_L), but their usefulness primarily relies on the selective scattering of phonons over charge carriers. Alternatively, crystalline solids innately exhibiting a low κ_L can constitute an attractive paradigm capable of offering the long-sought approach for decoupling electron and phonon transport to realize potential candidates for thermoelectric (TE) energy conversion. In this Perspective, we discuss the correlations between chemical bonding and lattice dynamics in specific materials and the ensuing characteristics underpinning an intrinsically low κ_L therein, viz., lattice anharmonicity, resonant bonding, intrinsic rattling, part-liquid states, and order−disorder transitions. Knowledge of these aspects should guide the discovery and design of new low-κ_L solids with potential TE applications.

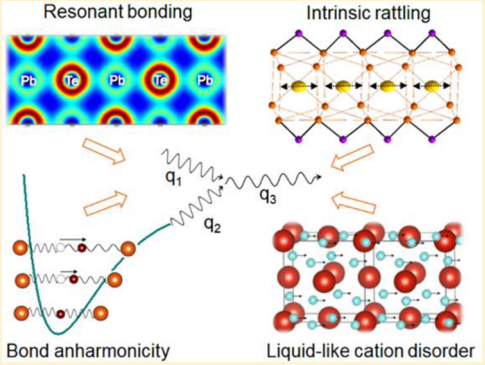

In light of burgeoning demand for energy, thermoelectric (TE) materials with a potential to convert temperature gradients into electricity are presumed to play a significant role in energy harvesting and management ancillary to photovoltaic materials. A surge in TE research over the past decade has led to the discovery of several high-performing TE materials and revealed various aspects governing a high TE efficiency.[1−3] From a materials perspective, the rationale for enhancing the TE efficiency lies in optimizing the electrical and thermal properties of a TE material and thereby the TE figure-of-merit, $zT = \sigma S^2 T/(\kappa_e + \kappa_L)$, where σ is the electrical conductivity, S is the Seebeck coefficient, κ_e and κ_L are the electronic and lattice thermal conductivities, respectively, and T is the absolute temperature. A strong correlation among the above parameters, as dictated by the Wiedemann−Franz law ($\kappa_e = L\sigma T$, where L is the temperature-dependent Lorentz number), imposes a fundamental limitation on the maximum zT achievable for a given TE material. Ongoing efforts in TE research are largely focused at (a) boosting the zT to a higher value close to 3 by further optimizing the current state-of-art TE materials and (b) exploring new materials preferably with nontoxic and abundant constituents and investigating the various aspects affecting their TE performance. zT is boosted by enhancing the power factor (σS^2) or/and reducing κ_L. Strategies to enhance σS^2 rely on tuning the concentration, effective mass, and mobility (m^*) of charge carriers through modification of the electronic band structure or density of states near the Fermi level via chemical doping or alloying.[4−6] On the other hand, κ_L is suppressed traditionally by means of hierarchical architectures where the atomic scale (e.g., point defects), nanoscale (e.g., endotaxial precipitates), and mesoscale (e.g., grain boundaries) defects in the host matrix lead to Rayleigh scattering of phonons with a broad range of wavelengths.[7−9] This extrinsic route to suppression of κ_L has been proven efficient notably for lead and tin chalcogenides.[10−12] However, in addition to phonon scattering by defects and nanostructuring, detrimental scattering of charge carriers is not entirely averted, limiting the overall zT in most other TE materials. In this respect, materials with intrinsically low κ_L are not only practically convenient but also serve as models to understand the correlation between chemical bonding and lattice dynamics impacting the phonon transport, a topic of fundamental interest in solid-state chemistry and materials science. Besides, the low-κ_L solids being of practical importance not only for TE applications but other industrial areas such as thermal barrier coatings necessitates extensive research on them.

Extrinsic defects can efficiently scatter a broad range of phonons, but solids innately exhibiting a low κ_L are convenient to mitigate an undesirable scattering of charge carriers by the defects.

Received: March 19, 2018
Accepted: May 4, 2018
Published: May 4, 2018

DOI: 10.1021/acsenergylett.8b00435
ACS Energy Lett. 2018, 3, 1315−1324

Slack had initially envisaged a "phonon-glass electron-crystal" (PGEC) wherein the phonon and electron transport channels are decoupled, thus facilitating independent control of phononic and electronic properties.[13] A PGEC crystal manifests a glass-like low κ_L, while the crystalline conduits to charge carriers provide for high electrical conductivity. The PGEC concept inspired several investigations and led to a significant increase in zT in caged compounds such as skutterudites and clathrates.[14,15] The latter can be incorporated with guest fillers that randomly rattle within the oversized voids, producing low-lying single-frequency optical vibrations characteristic of the guest atom. Multiple guest atoms when incorporated in the host produce a spectrum of such low-energy optical phonons that cause "resonant" scattering of the heat-carrying acoustic phonons of the host, thereby suppressing its κ_L. Simultaneously, these guest atoms serve as dopants to tune the carrier concentrations and enhance the TE power factor of the host. Both electropositive and electronegative guest atoms can be incorporated within the cages of the host framework, and the formation enthalpy (i.e., stability) of such inclusion compounds is governed by the electronegativity difference and specific nature of host−guest interactions.[15,16] Achieving a suitable material with properties akin to PGEC is key and indeed considered a holy grail of TE research today.

Heat is transported through quasiparticles called phonons that originate from lattice vibrations propagating through matter. Kinetic theory describes κ_L of a solid material as $\kappa_L = \frac{1}{3} C_V v_g^2 \tau$, where C_V is the specific heat capacity at constant volume, v_g is the group velocity of phonons, and τ is the phonon relaxation time. v_g is given by the slope of frequency vs k vector and is, therefore, material-dependent. Because $v_g \propto \left(\frac{f}{m}\right)^{1/2}$, where f and m denote, respectively, the force constant and mass, compounds with either weak chemical bonds or heavy constituent atoms will have a low v_g and hence κ_L. C_V is given by the partial derivative of total energy with respect to temperature and represents the total energy stored in excitations of phonons. A 3-D lattice with N number of unit cells and n number of atoms per unit cell will have $3n$ phonon branches and $3nN$ normal modes. Of the $3n$ phonon branches, 3 are acoustic branches and the rest $(3n - 3)$ are optical branches. As the optical branches are usually far higher in energy than the acoustic branches, C_V is usually dominated by the latter at low temperatures. Furthermore, the acoustic phonons due to their relatively high v_g have sole or dominant contribution to κ_L. Complex systems with large unit cells have a significant fraction of optical phonons that can be low-lying in energy close to the acoustic phonons, and a considerable fraction of heat is stored in these optical phonons whose contribution to κ_L can, however, be assumed negligible owing to their near-zero v_g. Therefore, complex materials particularly with heavy atoms constitute an effective paradigm for achieving a poor κ_L, and promising zT values had indeed been demonstrated earlier with appropriate engineering of electronic properties.[17] Besides, due to the proximity in energy, the optical phonons can couple with the heat-carrying acoustic phonons, leading to a low κ_L, and this is not limited to only the complex systems but also other materials with weak bonding characteristics, rattling dynamics, and soft optical phonons, as discussed below. Such an optical−acoustic coupling usually manifests as an avoided-crossing in the phonon dispersion and has an effect of reducing the group velocities of acoustic phonons as well as increasing the scattering phase space. Finally, τ can be reduced to an extent where the mean-free path ($l = v_g \cdot \tau$) of phonons can be as low as interatomic spacing by incorporating defects of varied dimensionality, which can scatter phonons with a broad range of wavelengths. Besides, there are always intrinsic phonon−phonon scatterings particularly pronounced at high temperatures due to lattice anharmonicity leading to a finite τ and κ_L.

Recent investigations of κ_L in certain TE materials have unveiled particular intrinsic phonon scattering phenomena beyond defect/boundary scattering and guest atom rattling, viz., strong lattice anharmonicity,[18,19] resonant bonding,[20,21] soft phonons,[22] intrinsic rattling,[23−27] bonding hierarchy, part-crystalline part-liquid states,[28] order−disorder transitions,[29−31] etc. (Figure 1). In this Perspective, we aim to provide a broader

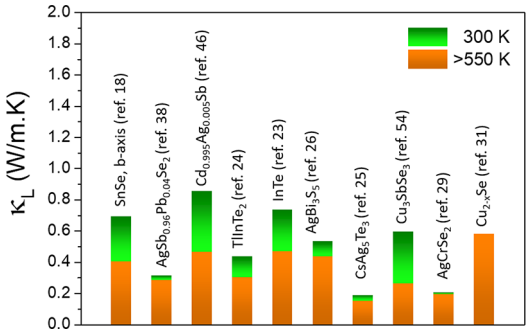

Figure 1. Histogram showing the experimental κ_L near 300 K and beyond 550 K for various compounds exhibiting an intrinsically low κ_L.

context to the said intrinsic phenomena and their associated mechanism(s) of suppressing κ_L, while underscoring the guiding principles for achieving a minimal κ_L in general. Finally, we present our opinions and a future outlook toward utilizing these concepts for exploring high-performing TE materials.

Anharmonicity and Phonon−Phonon Interactions. In a perfect harmonic oscillator, the interatomic force constant (k) does not depend on the displacement (x) of the atom away from its equilibrium position such that the force on each atom is $F(x) = kx$ and all of the allowed frequencies of such atomic vibrations depend only on k, the mass of atoms (m), and the propagation velocity (v) but not on x. Anharmonicity is a measure of how much a real crystal deviates from ideal harmonic behavior. In a real solid, the force is not linearly dependent on x such that k and allowed phonon frequencies become functions of x, as well as the interatomic distance and unit cell volume (V) of the crystal. The Gruneisen parameter, $\gamma(\omega) = \mathrm{d}\ln(\omega)/\mathrm{d}\ln(V)$, quantifies the anharmonicity for a given frequency (ω) of the phonon. Anharmonicity of the interatomic bonds drives the phonon−phonon Umklapp (U) and normal (N) scattering processes that intrinsically limit the κ_L at elevated temperatures, as first shown by Peierls,[32] with the probability of such phonon scattering processes being proportional to the average of γ^2 taken over all frequencies.[33] The momentum of interacting phonons is not conserved in an anharmonic U process, and a net loss of momentum causes κ_L to decay monotonically at high temperatures where U processes dominate.[19] Slack's model[34] predicts κ_L in the regime of three-phonon U scattering, assuming dominant heat transport by acoustic phonons as $\kappa_L = A(\bar{M}\theta_D^3\delta)/(\gamma^2 n^{2/3} T)$, where $\bar{M}$ is the average mass of the atoms in the crystal, θ_D is the Debye temperature, δ^3 is the volume per atom,

DOI: 10.1021/acsenergylett.8b00435
ACS Energy Lett. 2018, 3, 1315−1324

γ is the Grüneisen parameter, n is the number of atoms per primitive unit cell, T is temperature, and A is a physical constant ($\sim 3.1 \times 10^6$ if κ_L is in W/m·K, $\bar{M}$ in amu, and δ in Å). Whereas anharmonicity is a universal feature that renders κ_L of a crystalline solid a temperature-dependent finite quantity, strong anharmonicity in the lattice potential can significantly suppress κ_L, alleviating the need for artificial nanostructuring or alloying that usually degrades the electron mobility.

Strong lattice anharmonicity augments Umklapp phonon−phonon scatterings, suppressing the κ_L significantly.

Single-crystalline layered SnSe, a binary compound with light elements, is found to exhibit a record high $zT \approx 2.6$ with strongly anisotropic TE properties due to weak interlayer van der Waals bonding along the a-axis relative to strong intralayer covalent bonding in the $b-c$ plane (Figure 2a).[18] The high zT in SnSe stems mainly from its extremely low $\kappa_L < 1$ W/m·K (Figure 2d), which is indeed surprising owing to a common perception that low-κ_L materials usually possess either complex crystal structures or heavy constituent atoms. SnSe has a layered orthorhombic structure with two Sn−Se bilayers in the unit cell along the a-direction (Figure 2a). It exhibits a symmetry-lowering continuous transition from the *Cmcm* phase to the *Pnma* phase below $T_c \approx 810$ K accompanied by distortion in the local Sn coordination (Figure 2a). The phase transition is caused by lattice instability associated with the condensation of a soft transverse optic (TO) phonon mode at the Brillouin zone center.[21] Strong anharmonicity stems from Sn−Se bonds, especially the d2 and d3 bonds (Figure 2a), which induce cubic terms in the expansion of interatomic potential due to nonlinear forces.[21] The distortion corresponding to the cubic term overlaps with the said soft TO mode at the zone center, emphasizing the role of anharmonicity during the *Cmcm* to *Pnma* phase transition.[21] The phonon dispersion of SnSe shows soft acoustic modes especially along the crystallographic a-axis (Γ−X direction of the Brillouin zone) due to weak interatomic bonding along this direction (Figure 2b).[18] Besides, the calculated acoustic mode Gruneisen parameters (γ_i) are all large, being greater along the a-axis than those in other directions. The average γ values along a-, b-, and c-directions are 4.1, 2.1, and 2.3, respectively (Figure 2c).[18] The strong anharmonicity (i.e., large γ) originates from bonding instability inherent to SnSe. The latter arises due to large polarizabilities and long-range interatomic force constants associated with the resonant network of p-orbitals of Se atoms, coupled with local off-centring of Sn atoms caused by their active $5s^2$ lone pairs.[21] Resonant bonding is discussed further in the following section.

The importance of s^2 lone-pair orbitals in causing strong bond anharmonicity has also been emphasized in the rock-salt I−V−VI_2 (I = Ag/Cu/Alkali metals; V = Sb/Bi, VI = chalcogens) class (Figure 3a) of low- κ_L compounds.[19,35−39] The wave functions of the lone pairs (of group V cations) are extended and interact with the p-orbitals of chalcogen atoms with the extent of overlap scaling with bond ionicity. Beyond a threshold, this cation-s−anion-p interaction can drive structural distortion to a lower symmetry, thereby stabilizing the s^2 lone pairs. However, just below this threshold where the rock-salt structure is marginally stable, the s^2 orbitals can be very sensitive to small, local variations in bond distances such as those induced by lattice vibrations. As a consequence, bond strengths become extremely sensitive to these local distortions, i.e., the bonds become strongly anharmonic with anomalously high γ for the associated phonon modes. Using first-principles calculations, the electronic origin of the lattice anharmonicity has been illustrated for the rock-salt-based cation-ordered $NaSbSe_2$

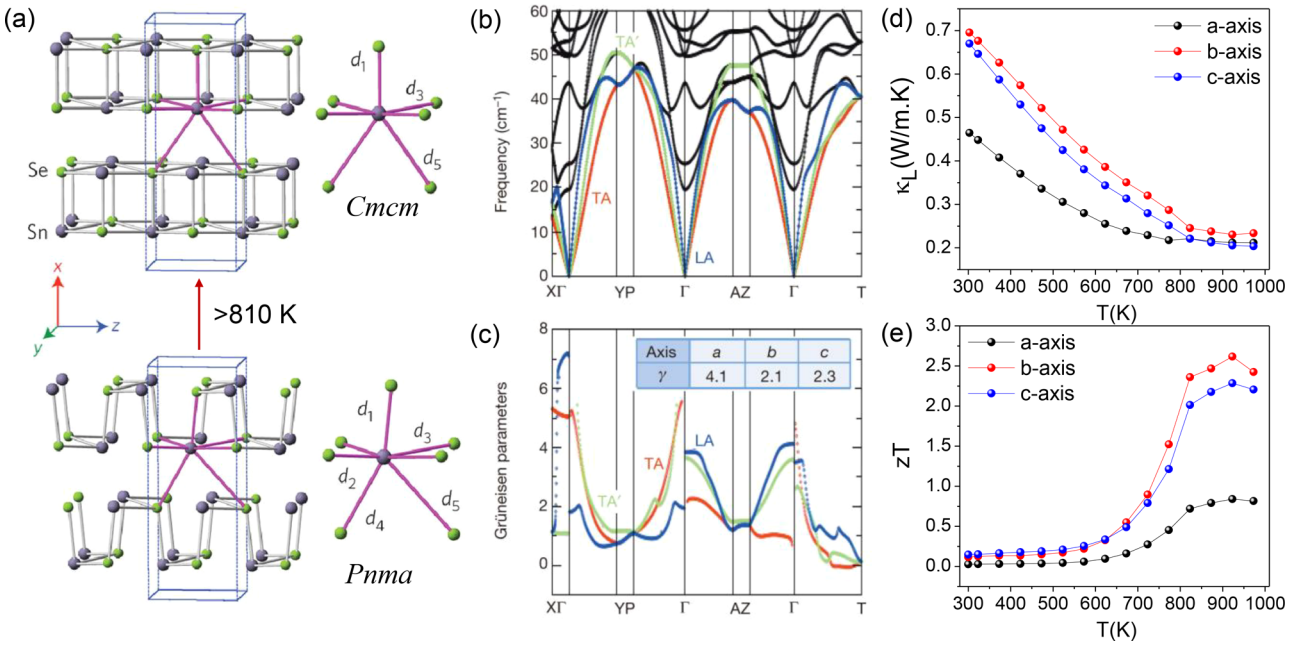

Figure 2. Schematic showing the structural transformation from *Pnma* to *Cmcm* phase of layered SnSe beyond 810 K and the associated change in $SnSe_7$ coordination polyhedron. The gray and green spheres denote Sn and Se atoms, respectively. Calculated (b) phonon dispersion and (c) mode Grüneisen parameter (γ) for the three acoustic branches of SnSe. TA′ and TA denote the two transverse acoustic phonon branches, whereas LA denotes the longitudinal acoustic phonon branch. The average γ values along a-, b-, and c-axes of a conventional unit cell are tabulated in the inset. Temperature-dependent (d) κ_L and (e) zT measured along the a-, b-, and c-axes of single-crystalline SnSe. Panel (a) is adapted from ref 21; (b−e) are adapted from ref 18. Copyright 2015 and 2014, Nature Publishing Group.

DOI: 10.1021/acsenergylett.8b00435
ACS Energy Lett. 2018, 3, 1315−1324

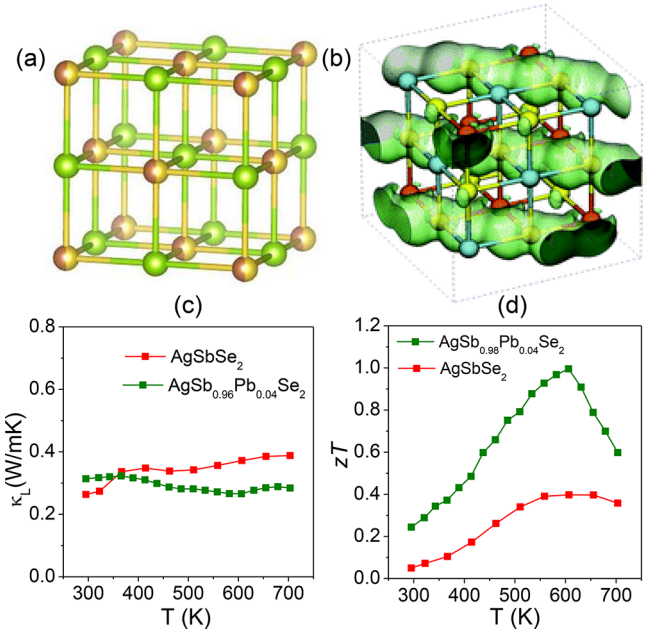

Figure 3. (a) Schematic of a disordered rock-salt crystal structure of I–V–VI_2 compounds. Group VI atoms are denoted by green spheres, whereas group I and V atoms are denoted by mixed spheres, indicating their random distribution. (b) Calculated polarization of $5s^2$ lone pairs of Sb atoms in rock-salt-based, cation-ordered $NaSbSe_2$ in response to Se displacements. Na, Sb, and Se atoms are denoted by blue, orange, and yellow spheres, respectively. (c) κ_L and (d) zT of $AgSbSe_2$ and 4 mol % Pb-doped $AgSbSe_2$ in the 300–700 K range. Panel (b) is reprinted from ref 19. Panels (c,d) are adapted from ref 38. Copyright 2013, Royal Society of Chemistry.

through strong polarization of Sb $5s^2$ lone pairs in response to Se displacements along the [1−10] direction (Figure 3b).[19] Notably, the condition for strong lattice anharmonicity in rock-salt I–V–VI_2 compounds borders on the threshold of structural collapse as the energetics of the s^2 lone pair dictates the strength of cation-s–anion-p interaction and hence the stability of the rock-salt structure in these and other related compounds.[40,41] A similar situation occurs for IV–VI compounds; as one moves from Ge to Pb, the ns^2 lone pair becomes increasingly stable due to relativistic effects and favors a stable rock-salt structure in PbTe whereas GeTe undergoes a rhombohedral distortion due to strong cation-s–anion-p interaction.[40] $AgSbSe_2$ with a disordered rock-salt structure is found to exhibit a high average γ value of ca. 3.7 owing to strong anharmonicity and an ultralow κ_L (<0.4 W/m·K) beyond 300 K (Figure 3c).[19,38] Thanks to the favorable valence band structure with multiple degenerate valleys, we have been able to significantly enhance the zT of $AgSbSe_2$ close to unity by appropriate carrier engineering via Pb doping (Figure 3d).[38] It is also worth noting that the cation site disorder in rock-salt $AgSbSe_2$ (Figure 3a) is not conducive to effective phonon transport owing to random fluctuations in the local force constants of Ag^+ and Sb^{3+} cations. Besides, there is also recent evidence of energetically favorable nanoscale domains of superstructures with locally ordered Ag and Bi/Sb cations in related rock-salt compounds such as $AgSbTe_2$[42] and AgBiSeS.[43] Likewise, the structural transitions in $AgBiS_2$ and $AgBiSe_2$ from disordered (rock-salt phase) to ordered polymorphs (trigonal or hexagonal) proceed through formation of ordered nanoscale domains and their subsequent growth.[44] These nanoscale domains can effectively scatter phonons in conjunction with bond anharmonicity, leading to a low κ_L (<1 W/m·K near 300 K).[36,37] Therefore, the low κ_L in this class of compounds should result from a combined effect of lone-pair-induced bond anharmonicity, cation disorder, and nanoscale inhomogeneities.

Resonant Bonding. The phonon lifetimes relate to the inverse of the three-phonon scattering cross section. A material with a low optical–acoustic phonon band gap will have a high cross section of anharmonic optical–acoustic phonon scattering, leading to a low κ_L. Rock-salt IV–VI compounds (e.g., lead chalcogenides and SnTe) as well as V_2–VI_3 materials (e.g., Bi_2Te_3) and V metals (e.g., Bi and Sb) with distorted rock-salt-based structures exhibit resonant bonding that leads to soft optical phonons.[20] These compounds have fewer valence electrons available per atom to form six two-center–two-electron (2c–2e) octahedral bonds. For example, PbTe with octahedrally coordinated Pb and Te atoms on average has three valence electrons (Pb:2, Te:4) per atom, while six electrons are required to form all six 2c–2e bonds. Coordination can, however, be satisfied by forming long-range resonance bonds or Zintl structures with cationic and anionic substructures. In rock-salt PbTe, three valence p electrons per atom on average have several possible choices of forming six octahedral bonds; a hybridization between all possible choices engenders resonant bonding, the extent of which weakens with distortion in the rock-salt structure as in Bi_2Te_3 or Bi.[20] Due to resonance bonding, the electron density distribution in PbTe is delocalized with long-range interactions between atoms along the ⟨100⟩ direction (Figure 4a, left panel). The electron polarization is, therefore, long-ranged, reaching even the fourth-nearest neighbor (Figure 4a, right panel). As a result, materials with resonant bonding usually exhibit long-range interatomic force constants and large electronic polarizabilities, dielectric constants, and Born charges. The significant feature of such resonant bonding is the presence of a soft TO phonon, which is deemed responsible for ferroelectric distortion in Ge- and Sn-doped PbTe upon cooling below a critical temperature.[45] In pristine PbTe, the soft TO phonon does not freeze down to zero frequency upon cooling, thus avoiding ferroelectric distortion, but the near-ferroelectric behavior causes a low κ_L due to strong anharmonic scattering of LA phonon modes by the soft TO phonon.[45] Figure 4b shows the phonon dispersion of PbTe at 300 K, experimentally determined by inelastic neutron scattering. It reveals an avoided crossing between LA and TO branches around q = (0/, 0/, 1/3) due to anharmonic repulsion between these modes, in contrast with the harmonic dispersions (shown as white solid lines) calculated by density functional theory (DFT).[45] The exceptional TE performance in PbTe stems from its low κ_L (~2.2 W/m·K at 300 K) in conjunction with its favorable electronic structure with multiple degenerate band valleys.[4]

Long-ranged interactions in electron-poor compounds cause highly polarizable bonds and soft phonons, driving anharmonic optical–acoustic scattering.

Orthorhombic CdSb is another example of an electron-deficient compound that forms multicenter bonds.[46] Investigations on atomic interactions in CdSb using electron density analysis and an electron-localizability indicator suggest a bonding scheme in CdSb as follows. Covalently bonded Sb–Sb dumbbells interconnected by 2c Cd–Sb bonds (Cd(3)–Sb and

DOI: 10.1021/acsenergylett.8b00435
ACS Energy Lett. 2018, 3, 1315–1324

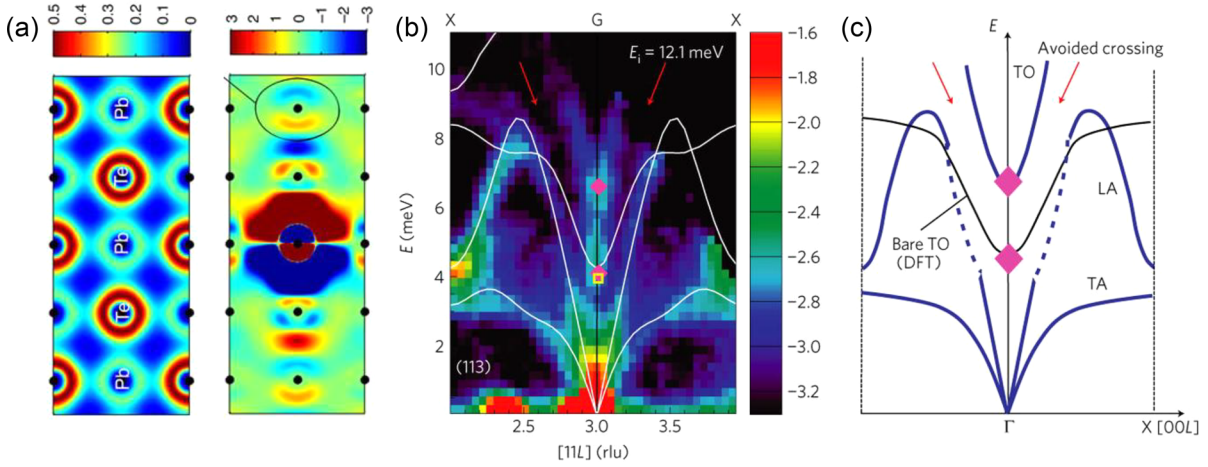

Figure 4. (a) Plots of the ground-state electron distribution in PbTe revealing largely delocalized electron density (left panel) and long-ranged electronic polarization induced by displacement of the center atom (right panel). Polarization reaching the fourth-nearest neighbor is shown in a circle. The plots are on the (100) plane, with each black dot representing an atom. The units are in $Å^{-3}$. (b) Phonon dispersions obtained from inelastic neutron scattering for PbTe at 300 K, showing the avoided crossing of LA and TO phonon branches. The harmonic dispersions calculated with the DFT are shown as white solid lines. (c) Schematic representation of (b) with the phonon dispersions as blue lines and the calculated bare TO branch as a solid black line. Red arrows in (b) and (c) point to the region of avoided-crossing of LA and TO modes. Panel (a) is adapted from ref 20; Panels (b) and (c) are reprinted from ref 45.Copyright 2014 and 2011, Nature Publishing Group.

Cd(4)−Sb) organize into 2-D layers running perpendicular to the [100] direction (Figure 5a−c). These layers are interconnected into a 3-D framework via 3c interactions (Cd(1)−Sb−Cd(2)), as shown in Figure 5c. The 3c bonding interactions in CdSb are driven by the electron demand (3.5 electrons per atom) relative to a system of tetrahedral coordination with four electrons per atom. The highly deformable electron density in such multicenter bonds leads to a large lattice anharmonicity and strong optical−acoustic coupling, thus resulting in a low κ_L (Figure 5d). By doping CdSb with Ag, its electrical properties have been enhanced to yield a maximum zT of ∼1.3 at 560 K for the 0.5 mol % Ag-doped CdSb (Figure 5d), which seems attractive for TE power generation at intermediate temperatures.

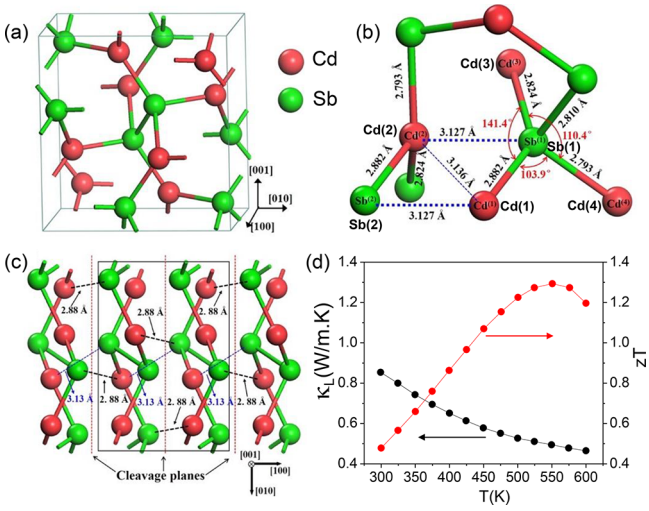

Figure 5. (a) Orthorhombic unit cell of CdSb showing bonds shorter than 3 Å. (b) Bonding environment for Cd and Sb atoms showing the various bond distances and angles. (c) Projection of structure along the [001] direction. The vertical dotted lines denote the cleavage planes containing the deformable 3c bonds. (d) κ_L and zT (300−660 K) plots for the 0.5 mol % Ag-doped CdSb. Adapted from ref 46. Copyright 2015, American Chemical Society.

Intrinsic Rattling Vibrations. In the context of guest atom rattling in filled skutterudites,[13] a local bonding asymmetry can drive anharmonic rattling vibrations enabled by the chemically active electron lone pairs in some compounds such as tetrahedrite $Cu_{12}Sb_4S_{13}$.[27] In comparison with caged compounds such as skutterudites, the Sb[CuS_3]Sb trigonal bipyramidal unit in $Cu_{12}Sb_4S_{13}$ can be viewed as a five-atom cage with a central Cu atom. Within the triangular CuS_3 plane, there are two strong and one intermediately strong Cu−S covalent bonds. Along the out-of-plane direction, a bonding fluctuation exists with weak bonding between Cu and either of the two Sb atoms enabled by the lone-pair electrons on Sb. The asymmetry in bonding along in-plane and out-of-plane directions of the Sb[CuS_3]Sb unit induces quasi-localized, large-amplitude anharmonic Cu vibrations akin to guest-rattling modes in skutterudites, which are likely the cause for low κ_L (0.61 W/m·K at 720 K) in $Cu_{12}Sb_4S_{13}$. zT has been optimized by doping/alloying Cu or S sites.[47] A maximum zT of ca. 1 has been achieved at 723 K by co-doping the Cu site with Ni and Zn.[48]

> Intrinsic rattling vibrations of weakly bonded constituents, occasionally enabled by lone pairs, induce anharmonic soft optical phonons that couple with the acoustic phonons.

Recently, we have shown Zintl-type $AInTe_2$ (A = In^+/Tl^+) compounds to exhibit very low κ_L values (0.4−0.8 W/m·K) in the 300−700 K range, which decay down to the theoretical amorphous limit at elevated temperatures (Figure 6e).[23,24] These compounds have tetragonal crystal structure (*I*4/*mmm* space group) featuring covalently bonded $(InTe_2)_n^{-n}$ anionic chains interlocked electrostatically with chains of Tl^+ or In^+ cations (Figure 6a). Each Tl^+ or In^+ is surrounded by eight Te ions (of the anionic substructure) in a distorted square-antiprismatic

DOI: 10.1021/acsenergylett.8b00435
ACS Energy Lett. 2018, 3, 1315−1324

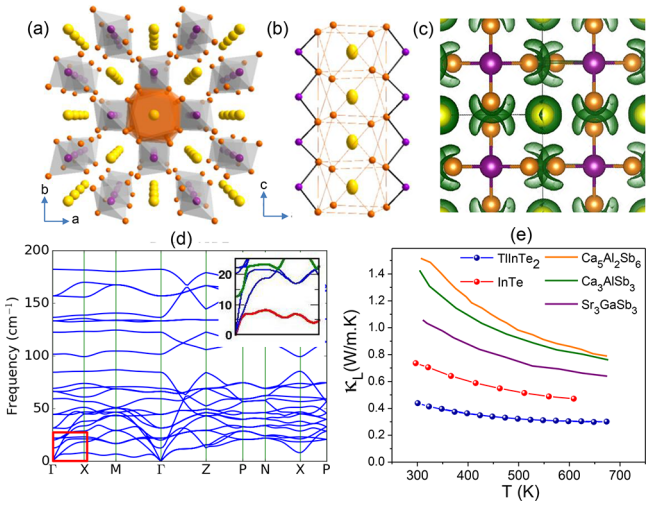

Figure 6. (a) Tetragonal crystal structure of $AInTe_2$ ($A = Tl^+/In^+$) Zintl compounds showing the chains of anionic (violet polyhedra) and cationic (orange polyhedron) substructures along the crystallographic *c*-axis. Purple, orange, and yellow spheres represent In^{3+}, Te^{2-}, and Tl^+/In^+ ions, respectively. (b) ADPs of Tl, In, and Te atoms in $TlInTe_2$ plotted as 80% probability ellipsoids. (c) Plot of the electron localization function showing a spherical distribution of $6s^2$ lone pairs of Tl^+ cations in $TlInTe_2$. The color codes of atoms in (b) and (c) are same as those in (a). (d) Calculated phonon dispersion of $TlInTe_2$. The zoomed region in the inset shows an avoided crossing between green and red branches near the Γ-point due to optical−acoustic coupling. (e) Experimental κ_L of InTe (ref 23) and $TlInTe_2$ (ref 24) compared with that of 1-D Zintl compounds, viz., $Ca_5Al_2Sb_6$ (ref 49), Ca_3AlSb_3 (ref 50), and Sr_3GaSb_3 (ref 51). Panels (b−d) are reprinted from ref 24. Copyright 2017, American Chemical Society.

arrangement through electrostatic interactions, whereas In^{3+} forms strong tetrahedral covalent bonds with Te ions. The weakly bound Tl^+/In^+ cations are characterized by large and anisotropic atomic displacement parameters (ADPs) especially along the *c*-axis ($U_{3,3} \approx 0.07$ Å^2 for Tl^+ at 300 K), akin to guest rattlers in skutterudites (Figure 6b). Notably, these large ADPs are in contrast with small (<0.015 Å^2) and isotropic ADPs associated with the cations in analogous complex (26−56 atoms per unit cell) 1-D Zintl compounds such as Ca_3AlSb_3, $Ca_5Al_2Sb_6$, and Sr_3GaSb_3.[49−51] $TlInTe_2$ and InTe indeed exhibit a lower κ_L compared with the above complex Zintl compounds (Figure 6e). Besides, the first-principles calculations reveal a spherical electron localization around Tl^+ or In^+ cation associated with the $6s^2$ or $5s^2$ lone pairs, respectively (Figure 6c). It has been shown earlier that a spherically distributed lone pair is unstable and forms a localized lobe by distorting the structure in the extreme case, as in perovskite $BiMnO_3$.[52] The said tetragonal $AInTe_2$ compounds, however, do not exhibit any apparent structural transitions in the 2−700 K range, though lone-pair-induced local off-centering of cations is possible similar to what had been observed earlier in the rock-salt PbTe.[53] While it necessitates further investigation, the situation can be viewed akin to the case of I−V−VI_2 rock-salt compounds where the phonons become extremely anharmonic in the absence of a lone-pair-driven distortion of the average structure. Therefore, in addition to thermal agitation, the propensity of the ns^2 lone pair of Tl^+/In^+ to stereochemically express itself plausibly augments the displacements of these cations along the *c*-axis, which are reflected as large ADPs. The intrinsic rattling dynamics of cations results in strongly anharmonic (with anomalously high mode γ) low-energy optical vibrations that manifest as Einstein modes in the low-temperature specific heat capacity. These optical modes, while not effective for heat transport due to their low group velocities, can couple with the heat-carrying acoustic phonons, as also revealed by the first-principles calculations (Figure 6d), and cause a low κ_L in these materials. Thus, the cation lone pairs play a role in suppressing the κ_L by inducing large cation displacements and anharmonicity. By optimizing the hole concentrations through In deficiencies, we have achieved a maximum zT of ca. 0.9 at 600 K for the ingots of nominal 0.3 mol % In-deficient InTe.[23]

An exceptionally low κ_L of 0.18 W/m·K at 300 K in $CsAg_5Te_3$ has been similarly attributed to anharmonic, concerted rattling of a group of Ag cations.[25] In $AgBi_3S_5$, a low κ_L of 0.3−0.5 W/m·K in the 300−800 K range arises due to double-rattling phonon modes associated with Ag and Bi vibrations.[26] Again, owing to a low κ_L, zT values of 1.5 (727 K) and 1 (800 K) have been achieved in $CsAg_5Te_3$ and 0.33% Cl-doped $AgBi_3S_5$, respectively.[25,26]

Part-Crystalline Part-Liquid States. In the above compounds, there exists a chemical bonding hierarchy in which the weakly bound constituent atoms exhibit local rattling dynamics. On the other hand, specific materials with a chemical bonding hierarchy as exemplified by Cu_3SbSe_3 can manifest a thermally induced "liquid-like" flow of a set of weakly bonded atoms resulting in a part-crystalline, part-liquid state.[28] Liquid-like dynamics of these atoms cause large thermal ADPs and manifest as collective soft vibrations leading to rattle-like thermal damping and, hence, a very low κ_L. Qiu et al. revealed through molecular dynamics simulations the diffusive and dynamic fluctuations of a set of copper atoms (Cu1z and Cu2xy) in Cu_3SbSe_3.[28] Interestingly, another school of thought has long attributed the low κ_L in Cu_3SbSe_3 to the Sb lone pair rendering Sb−Se bonds strongly anharmonic.[33] Qiu et al., however, associate the low κ_L with a rattle-like thermal damping (i.e., resonant scattering of acoustic phonons by rattling phonon modes) on the account of their small calculated γ values along with an apparent deviation in the temperature dependence of κ_L from calculations assuming a dominant anharmonic phonon scattering.[28] Though the jury seems to be still out, it is reasonable to consider the combined effect of lone pairs and the diffusive dynamics of Cu atoms in causing a low κ_L (0.6 W/m·K at 300 K) of Cu_3SbSe_3.[54]

> Dynamic fluctuations of a group of atoms in the lattice can cause part-crystalline, part-liquid states, leading to phonon damping.

Order−Disorder Transitions. In the high-temperature rock-salt phases of $Cu_{2-\delta}X$ (X = Se/S)[31,55,56] and their derivatives, such as AgCuX (X = S, Se, Te),[22,57] the cation sublattice completely "melts" above a transition temperature, imparting superionic liquid-like motion to the cations. The said compounds thus feature a rigid anion sublattice providing crystalline conduits for the charge carriers coexisting with a kinetically disordered cation sublattice. For example, the calculated phonon dispersion of the room-temperature orthorhombic phase of AgCuS (Figure 7a) features high- and low-energy phonon bands associated with the rigid anion and soft cation sublattices, respectively, with a distinct gap separating the two (Figure 7b).[57] Interestingly,

DOI: 10.1021/acsenergylett.8b00435
ACS Energy Lett. 2018, 3, 1315−1324

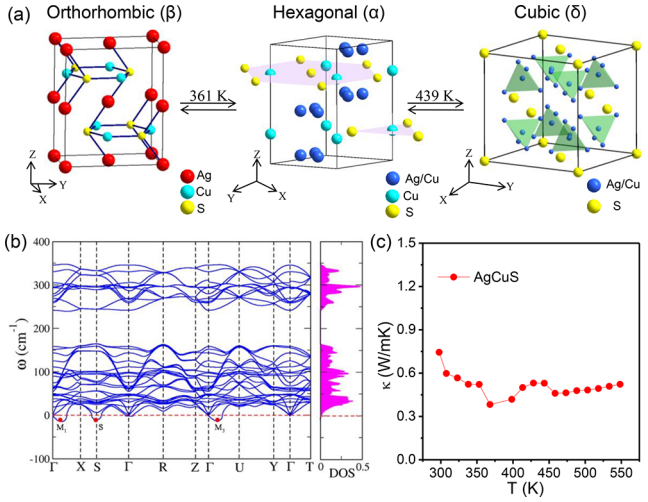

Figure 7. (a) Structural transformation of AgCuS with temperature. The Ag and Cu atoms are ordered in the room-temperature orthorhombic (β) structure, while they are disordered and superionic in the high-temperature cubic (δ) structure. (b) Plots of the phonon dispersion and phonon density of states of β-AgCuS. (c) Temperature-dependent κ ($\approx\kappa_L$) of AgCuS. Adapted from ref 57. Copyright 2014, American Chemical Society.

such a phononic bandgap is reminiscent of an artificial phononic crystal where the periodic modulation of density and elastic properties leads to a variable phononic band gap as a means to manipulate thermal transport. The weak instabilities in the acoustic branch at M1, M3, and S points of the phonon dispersion in Figure 7b are related to shear deformation of atoms, and these along with several soft phonons ($\omega < 50$ cm^{-1}) result in a low κ_L of ~0.7 at 300 K in AgCuS (Figure 7c). At elevated temperatures, the dynamics and renormalization of these shear modes and cation-induced low-energy phonon modes plausibly drive the superionic structural transitions (Figure 7a) observed experimentally.[57] Recently, we have observed AgCuTe to exhibit an ultralow κ_L of ca. 0.35 W/m·K at 300 K and a remarkable zT of ca. 1.6 at 670 K.[22] AgCuTe exhibits a reversible, first-order hexagonal-to-rock-salt superionic transition beyond 470 K, which is associated with the disordering of its cation sublattice. Although the observed electrical properties of AgCuTe vary significantly across the superionic transition, κ_L remains low throughout the temperature range studied. Our first-principles studies indicate that hierarchical bond strengths, Ag-dominated soft optical modes, and an optical–acoustic coupling likely cause a low κ_L in the room-temperature hexagonal phase, while the kinetic disorder of Ag/Cu cations leads to reduced frequencies and mean-free paths of phonons in the high-temperature disordered rock-salt phase.

The cation sublattice "melting" can reduce not only the phonon mean-free path but also some of the heat-carrying TA vibrational modes, thereby suppressing the overall thermal transport. This picture complies with the fact that liquids with only longitudinal vibrational modes are less thermally conductive than solids with both transverse and longitudinal vibrational modes. The heat capacity of a crystalline solid saturates to the classical Dulong–Petit value ($3k_B$/atom) at elevated temperatures. The high-temperature specific heat in materials with a substantial liquid-like motion of ions such as $Cu_{2-x}Se$ is reduced to $2k_B$/atom due to lower vibrational degrees, thus resulting in a κ_L as low as 0.58 W/m·K at 600 K.[31] As a result, zT approaches ca. 1.5 at 1000 K in $Cu_{2-x}Se$.[31] Some of the above superionic TE compounds such as $Cu_{2-x}Se$ and AgCuTe have electrical conductivities typical of a degenerate semiconductor owing to intrinsic cation vacancies. Despite the disorder in the cation sublattice, the crystalline pathways due to the rigid anion sublattice can result in reasonable electrical conductivities observed for the high-temperature disordered phases. The possible interactions of charge carriers with diffusing cations are, however, not explicitly investigated hitherto.

Another example for liquid-like thermal conduction in a crystalline solid is $AgCrSe_2$.[30] It has a layered hexagonal structure at low temperatures constituting alternating layers of $CrSe_6$ octahedra and Ag ions stacked along the c-axis. Ag ions have two similar tetrahedral interstitial sites, one of which is completely occupied at low temperatures. As the temperature rises, there is an order–disorder transition in the occupation of Ag ions with 50% occupation of each of the sites. The low-lying intense TA phonons that are dominated by motions of Ag atoms are completely suppressed above the transition temperature where their lifetime is shorter than the relaxation time of local fluctuations, but the LA mode persists. This results in liquid-like thermal conduction with an extremely low κ_L of ca. 0.2 W/m·K at 500 K.[29] Despite a low TE power factor, the low κ_L leads to a reasonably high zT close to unity at 523 K in $AgCrSe_2$.[29]

> Order–disorder transitions at a sublattice level can lead to liquid-like thermal conduction in an otherwise crystalline solid.

We close our discussion on low-κ_L materials with the case of MgAgSb where multiple factors suppress κ_L. MgAgSb exhibits complex phase transitions with an α phase at room temperature and β and γ phases at intermediate (560–630 K) and high (630–700 K) temperatures, respectively. The tetragonal α-MgAgSb has a very complex crystal structure (24 atoms per primitive unit cell) comprising the distorted rock-salt lattice of Mg and Sb atoms, with the Ag atoms filling the voids thereof. Besides, the Mg–Ag–Sb three-center bonding leads to low-lying optical phonons that in turn cause a rattle-like thermal damping.[58] These factors together with intrinsic Ag vacancies result in a low κ_L of ca. 0.54 W/m·K at 300 K, and a maximum zT of ca. 1.3 has been achieved in α-MgAgSb at 550 K by controlling the Ag vacancies.[59]

Summary and Future Outlook. Materials with intrinsically low κ_L are practically advantageous with respect to extrinsic approaches of manipulating phonon transport via multiple defects as the latter largely rely on a high scattering rate of phonons relative to charge carriers. The intrinsic attributes of a low-κ_L solid are low acoustic group velocities (i.e., sound velocities), small phonon relaxation time (i.e., high phonon scattering rate), and small fraction of acoustic C_V (as in complex TE materials with a high proportion of low-energy optical modes). In general, a small energy gap between the acoustic and optical phonons favors strong coupling between the two, which lowers the sound velocities and increases the phonon scattering cross section. The soft optical phonons can arise due to several factors, as discussed above. The strong correlation between the chemical bonding and lattice dynamics impacting the phonon transport is apparent from the above discussion. Some of the intrinsic causes underlying a low κ_L are based on lattice anharmonicity originating from stereochemically active

DOI: 10.1021/acsenergylett.8b00435
ACS Energy Lett. 2018, 3, 1315–1324

lone pairs, resonant/multicenter bonding, and ferroelectric instability, whereas the rest stem from hierarchical bond strengths (i.e., the coexistence of rigid and fluctuating constituents) and order−disorder transitions. Although a few representative examples are discussed here, many other low-κ_L materials have been discovered to similarly exhibit the said intrinsic phenomena. Generally, routes to optimize electronic properties are less likely to affect the low κ_L in these materials unless the elastic properties are dramatically modified. To this end, low-κ_L solids can offer independent ways to optimize the electronic properties.

Analysis of bonding environments, ADPs, thermal expansion, and specific heat capacity can serve to predict a low κ_L in crystalline solids. Theoretical descriptors such as Grüneisen parameters, electron localization functions, dielectric constants, and Born charges also inform mechanisms leading to a low κ_L, and the first-principles phonon calculations form an integral part of discovering low-κ_L materials. Advanced experimental methods such as inelastic neutron scattering and analysis of the X-ray pair distribution function can determine the momentum-dependent phonon dispersions and evolution of local structure, respectively, as functions of temperature, which can provide critical pieces of information to rationalize a low κ_L. These in conjunction with powerful first-principles simulations are becoming increasingly handy to explore low-κ_L materials.

The current understanding of the said mechanisms should guide the exploration of new materials with an intrinsically low κ_L, but the obvious yet important question is whether they all possess promising TE performance. Essentially, they must also maintain a favorable electronic structure and facilitate carrier and/or band engineering in order to achieve significant TE power factors (σS^2), and therefore, an effective screening approach to realize the potential candidates is required. To this end, machine-learning-based engines are being developed under a material informatics project for rapid screening of hundreds of known TE compounds and predicting the feasibility and potential of user-designed TE compounds. However, importantly, potential TE materials should also possess stable performance and mechanical robustness for reliable and durable operation in devices. Unfortunately, low-κ_L materials with diffusive atomic dynamics (particularly the Ag- and Cu-containing compounds) are prone to degradation in TE properties as the atoms diffuse out of the structure, and those with order−disorder structural transitions can develop strain (cracks) across large temperature gradients, thus posing practical challenges from a device perspective. A search for new low-κ_L compounds overcoming the said challenges is, therefore, indispensable to realize efficient TE devices. Unlike how it may appear, the insights discussed here should not only guide the discovery of new low-κ_L compounds but also engineer phonon transport by rational design. For example, lone-pair-containing constituents can be deliberately incorporated to induce strong bond anharmonicity. Through appropriate substitution or alloying, the bond strengths, anharmonicity, and other elastic properties can be modified to suppress κ_L. Nonetheless, some of the above low-κ_L compounds demonstrate good stability and promising zT values, with single-crystalline SnSe currently holding a record high zT of 2.6 at mid-high temperatures. This is a significant discovery away from the toxic lead chalcogenides, which are otherwise posited to be champion materials in the TE community. We are hopeful that new insights are developed and many state-of-the-art TE materials exhibiting a low-κ_L and high zT are unravelled in the near future.

AUTHOR INFORMATION

Corresponding Author

*E-mail: kanishka@jncasr.ac.in.

ORCID

Kanishka Biswas: 0000-0001-9119-2455

Notes

The authors declare no competing financial interest.

Biographies

Manoj K. Jana received a Ph.D. degree (2017) in chemical sciences from the New Chemistry Unit, Jawaharlal Nehru Centre for Advanced Scientific Research (JNCASR), Bangalore under the guidance of C. N. R. Rao and Kanishka Biswas. His Ph.D. research mainly pertains to structure−property relationships in layered transition metal dichalcogenides and thermoelectric materials with low thermal conductivity. He is currently a postdoctoral fellow pursuing research on organic−inorganic hybrid perovskites under the guidance of David Mitzi at the Department of Mechanical Engineering and Materials Science, Duke University, NC, U.S.A.

Kanishka Biswas obtained M.S. and Ph.D. degrees from the Solid State Structural Chemistry Unit, Indian Institute of Science, Bangalore (2009) under the supervision of C. N. R. Rao and did postdoctoral research with Mercouri G. Kanatzidis at the Department of Chemistry, Northwestern University (2009−2012). He is an Assistant Professor in the New Chemistry Unit, Jawaharlal Nehru Centre for Advanced Scientific Research (JNCASR), Bangalore. He is pursuing research in the solid-state inorganic chemistry of metal chalcogenides and halides, thermoelectrics, topological materials, 2D materials, and water purification (http://www.jncasr.ac.in/kanishka/).

ACKNOWLEDGMENTS

M.K.J. thanks CSIR-India for a research fellowship. We thank SERB, DST (EMR/2016/000651), DAE BRNS-YSRA [37(3)/20/01/2015/BRNS], and Sheikh Saqr Laboratory for supporting thermoelectric research in our lab.

REFERENCES

(1) Ge, Z.-H.; Zhao, L.-D.; Wu, D.; Liu, X.; Zhang, B.-P.; Li, J.-F.; He, J. Low-cost, abundant binary sulfides as promising thermoelectric materials. *Mater. Today* **2016**, *19*, 227−239.

(2) Tan, G.; Zhao, L.-D.; Kanatzidis, M. G. Rationally designing high-Performance bulk thermoelectric materials. *Chem. Rev.* **2016**, *116*, 12123−12149.

(3) Zhao, L.-D.; Dravid, V. P.; Kanatzidis, M. G. The panoscopic approach to high performance thermoelectrics. *Energy Environ. Sci.* **2014**, *7*, 251−268.

(4) Pei, Y.; Shi, X.; LaLonde, A.; Wang, H.; Chen, L.; Snyder, G. J. Convergence of electronic bands for high performance bulk thermoelectrics. *Nature* **2011**, *473*, 66−69.

(5) Li, W.; Wu, Y.; Lin, S.; Chen, Z.; Li, J.; Zhang, X.; Zheng, L.; Pei, Y. Advances in environment-friendly SnTe thermoelectrics. *ACS Energy Lett.* **2017**, *2*, 2349−2355.

(6) Banik, A.; Shenoy, U. S.; Saha, S.; Waghmare, U. V.; Biswas, K. High power factor and enhanced thermoelectric performance of SnTe-$AgInTe_2$: Synergistic effect of resonance level and valence band convergence. *J. Am. Chem. Soc.* **2016**, *138*, 13068−13075.

(7) Vineis, C. J.; Shakouri, A.; Majumdar, A.; Kanatzidis, M. G. Nanostructured thermoelectrics: Big efficiency gains from small features. *Adv. Mater.* **2010**, *22*, 3970−3980.

(8) Biswas, K.; He, J.; Zhang, Q.; Wang, G.; Uher, C.; Dravid, V. P.; Kanatzidis, M. G. Strained endotaxial nanostructures with high thermoelectric figure of merit. *Nat. Chem.* **2011**, *3*, 160−166.

(9) Samanta, M.; Biswas, K. Low thermal conductivity and high thermoelectric performance in $(GeTe)_{1-2x}(GeSe)_x(GeS)_x$: competi-

DOI: 10.1021/acsenergylett.8b00435
ACS Energy Lett. 2018, 3, 1315−1324

tion between solid solution and phase separation. *J. Am. Chem. Soc.* **2017**, *139*, 9382−9391.
(10) Banik, A.; Vishal, B.; Perumal, S.; Datta, R.; Biswas, K. The origin of low thermal conductivity in $Sn_{1-x}Sb_xTe$: phonon scattering via layered intergrowth nanostructures. *Energy Environ. Sci.* **2016**, *9*, 2011−2019.
(11) Wu, H.; Chang, C.; Feng, D.; Xiao, Y.; Zhang, X.; Pei, Y.; Zheng, L.; Wu, D.; Gong, S.; Chen, Y.; et al. Synergistically optimized electrical and thermal transport properties of SnTe via alloying high-solubility MnTe. *Energy Environ. Sci.* **2015**, *8*, 3298−3312.
(12) Biswas, K.; He, J.; Blum, I. D.; Wu, C.-I.; Hogan, T. P.; Seidman, D. N.; Dravid, V. P.; Kanatzidis, M. G. High-performance bulk thermoelectrics with all-scale hierarchical architectures. *Nature* **2012**, *489*, 414−418.
(13) Slack, G. A. *CRC handbook of thermoelectrics*; CRC Press: New York, 1995, 407−440.
(14) Takabatake, T.; Suekuni, K.; Nakayama, T.; Kaneshita, E. Phonon-glass electron-crystal thermoelectric clathrates: Experiments and theory. *Rev. Mod. Phys.* **2014**, *86*, 669−716.
(15) Shi, X.; Yang, J.; Salvador, J. R.; Chi, M.; Cho, J. Y.; Wang, H.; Bai, S.; Yang, J.; Zhang, W.; Chen, L. Multiple-filled skutterudites: High thermoelectric figure of merit through separately optimizing electrical and thermal transports. *J. Am. Chem. Soc.* **2011**, *133*, 7837−7846.
(16) Duan, B.; Yang, J.; Salvador, J. R.; He, Y.; Zhao, B.; Wang, S.; Wei, P.; Ohuchi, F. S.; Zhang, W.; Hermann, R. P.; et al. Electronegative guests in $CoSb_3$. *Energy Environ. Sci.* **2016**, *9*, 2090−2098.
(17) Snyder, G. J.; Toberer, E. S. Complex thermoelectric materials. *Nat. Mater.* **2008**, *7*, 105−114.
(18) Zhao, L.-D.; Lo, S.-H.; Zhang, Y.; Sun, H.; Tan, G.; Uher, C.; Wolverton, C.; Dravid, V. P.; Kanatzidis, M. G. Ultralow thermal conductivity and high thermoelectric figure of merit in SnSe crystals. *Nature* **2014**, *508*, 373−377.
(19) Nielsen, M. D.; Ozolins, V.; Heremans, J. P. Lone pair electrons minimize lattice thermal conductivity. *Energy Environ. Sci.* **2013**, *6*, 570−578.
(20) Lee, S.; Esfarjani, K.; Luo, T.; Zhou, J.; Tian, Z.; Chen, G. Resonant bonding leads to low lattice thermal conductivity. *Nat. Commun.* **2014**, *5*, 3525.
(21) Li, C. W.; Hong, J.; May, A. F.; Bansal, D.; Chi, S.; Hong, T.; Ehlers, G.; Delaire, O. Orbitally driven giant phonon anharmonicity in SnSe. *Nat. Phys.* **2015**, *11*, 1063−1069.
(22) Roychowdhury, S.; Jana, M. K.; Pan, J.; Guin, S. N.; Sanyal, D.; Waghmare, U. V.; Biswas, K. Soft phonon modes leading to ultralow thermal conductivity and high thermoelectric Performance in AgCuTe. *Angew. Chem., Int. Ed.* **2018**, *57*, 4043.
(23) Jana, M. K.; Pal, K.; Waghmare, U. V.; Biswas, K. The origin of ultralow thermal conductivity in InTe: Lone-pair-induced anharmonic rattling. *Angew. Chem., Int. Ed.* **2016**, *55*, 7792−7796.
(24) Jana, M. K.; Pal, K.; Warankar, A.; Mandal, P.; Waghmare, U. V.; Biswas, K. Intrinsic rattler-induced low thermal conductivity in Zintl type $TlInTe_2$. *J. Am. Chem. Soc.* **2017**, *139*, 4350−4353.
(25) Lin, H.; Tan, G.; Shen, J.-N.; Hao, S.; Wu, L.-M.; Calta, N.; Malliakas, C.; Wang, S.; Uher, C.; Wolverton, C.; et al. Concerted rattling in $CsAg_5Te_3$ leading to ultralow thermal conductivity and high thermoelectric performance. *Angew. Chem., Int. Ed.* **2016**, *55*, 11431−11436.
(26) Tan, G.; Hao, S.; Zhao, J.; Wolverton, C.; Kanatzidis, M. G. High thermoelectric performance in electron-Doped $AgBi_3S_5$ with ultralow thermal conductivity. *J. Am. Chem. Soc.* **2017**, *139*, 6467−6473.
(27) Lai, W.; Wang, Y.; Morelli, D. T.; Lu, X. From bonding asymmetry to anharmonic rattling in $Cu_{12}Sb_4S_{13}$ Tetrahedrites: When lone-pair electrons are not so lonely. *Adv. Funct. Mater.* **2015**, *25*, 3648−3657.
(28) Qiu, W.; Xi, L.; Wei, P.; Ke, X.; Yang, J.; Zhang, W. Part-crystalline part-liquid state and rattling-like thermal damping in materials with chemical-bond hierarchy. *Proc. Natl. Acad. Sci. U. S. A.* **2014**, *111*, 15031−15035.
(29) Gascoin, F.; Maignan, A. Order−disorder transition in $AgCrSe_2$: a new route to efficient thermoelectrics. *Chem. Mater.* **2011**, *23*, 2510−2513.
(30) Li, B.; Wang, H.; Kawakita, Y.; Zhang, Q.; Feygenson, M.; Yu, H. L.; Wu, D.; Ohara, K.; Kikuchi, T.; Shibata, K.; et al. Liquid-like thermal conduction in intercalated layered crystalline solids. *Nat. Mater.* **2018**, *17*, 226−230.
(31) Liu, H.; Shi, X.; Xu, F.; Zhang, L.; Zhang, W.; Chen, L.; Li, Q.; Uher, C.; Day, T.; Snyder, G. J. Copper ion liquid-like thermoelectrics. *Nat. Mater.* **2012**, *11*, 422−425.
(32) Peierls, R. Zur kinetischen theorie der wärmeleitung in kristallen. *Ann. Phys.* **1929**, *395*, 1055−1101.
(33) Zhang, Y.; Skoug, E.; Cain, J.; Ozoliņš, V.; Morelli, D.; Wolverton, C. First-principles description of anomalously low lattice thermal conductivity in thermoelectric Cu-Sb-Se ternary semiconductors. *Phys. Rev. B: Condens. Matter Mater. Phys.* **2012**, *85*, 054306.
(34) Slack, G. A. *Solid state physics*; Academic Press: Cambridge, MA, 1979, *34*, 1−71.
(35) Morelli, D. T.; Jovovic, V.; Heremans, J. P. Intrinsically minimal thermal conductivity in cubic I-V-VI_2 semiconductors. *Phys. Rev. Lett.* **2008**, *101*, 035901.
(36) Guin, S. N.; Srihari, V.; Biswas, K. Promising thermoelectric performance in n-type $AgBiSe_2$: effect of aliovalent anion doping. *J. Mater. Chem. A* **2015**, *3*, 648−655.
(37) Guin, S. N.; Biswas, K. Cation disorder and bond anharmonicity optimize the thermoelectric properties in kinetically stabilized rocksalt $AgBiS_2$ nanocrystals. *Chem. Mater.* **2013**, *25*, 3225−3231.
(38) Guin, S. N.; Chatterjee, A.; Negi, D. S.; Datta, R.; Biswas, K. High thermoelectric performance in tellurium free p-type $AgSbSe_2$. *Energy Environ. Sci.* **2013**, *6*, 2603−2608.
(39) Guin, S. N.; Banerjee, S.; Sanyal, D.; Pati, S. K.; Biswas, K. Nanoscale stabilization of nonequilibrium rock Salt BiAgSeS: Colloidal synthesis and temperature driven unusual phase transition. *Chem. Mater.* **2017**, *29*, 3769−3777.
(40) Waghmare, U. V.; Spaldin, N. A.; Kandpal, H. C.; Seshadri, R. First-principles indicators of metallicity and cation off-centricity in the IV-VI rocksalt chalcogenides of divalent Ge, Sn, and Pb. *Phys. Rev. B: Condens. Matter Mater. Phys.* **2003**, *67*, 125111.
(41) Walsh, A.; Payne, D. J.; Egdell, R. G.; Watson, G. W. Stereochemistry of post-transition metal oxides: revision of the classical lone pair model. *Chem. Soc. Rev.* **2011**, *40*, 4455−4463.
(42) Ma, J.; Delaire, O.; May, A. F.; Carlton, C. E.; McGuire, M. A.; VanBebber, L. H.; Abernathy, D. L.; Ehlers, G.; Hong, T.; Huq, A.; et al. Glass-like phonon scattering from a spontaneous nanostructure in $AgSbTe_2$. *Nat. Nanotechnol.* **2013**, *8*, 445.
(43) Pei, Y.-L.; Wu, H.; Sui, J.; Li, J.; Berardan, D.; Barreteau, C.; Pan, L.; Dragoe, N.; Liu, W.-S.; He, J.; et al. High thermoelectric performance in n-type BiAgSeS due to intrinsically low thermal conductivity. *Energy Environ. Sci.* **2013**, *6*, 1750−1755.
(44) Manolikas, C.; Spyridelis, J. Electron microscopic study of polymorphism and defects in $AgBiSe_2$ and $AgBiS_2$. *Mater. Res. Bull.* **1977**, *12*, 907−913.
(45) Delaire, O.; Ma, J.; Marty, K.; May, A. F.; McGuire, M. A.; Du, M. H.; Singh, D. J.; Podlesnyak, A.; Ehlers, G.; Lumsden, M. D.; et al. Giant anharmonic phonon scattering in PbTe. *Nat. Mater.* **2011**, *10*, 614−619.
(46) Wang, S.; Yang, J.; Wu, L.; Wei, P.; Yang, J.; Zhang, W.; Grin, Y. Anisotropic multicenter bonding and high thermoelectric performance in electron-poor CdSb. *Chem. Mater.* **2015**, *27*, 1071−1081.
(47) Chetty, R.; Bali, A.; Mallik, R. C. Tetrahedrites as thermoelectric materials: an overview. *J. Mater. Chem. C* **2015**, *3*, 12364−12378.
(48) Lu, X.; Morelli, D. T.; Xia, Y.; Ozolins, V. Increasing the thermoelectric figure of merit of tetrahedrites by co-doping with nickel and zinc. *Chem. Mater.* **2015**, *27*, 408−413.

DOI: 10.1021/acsenergylett.8b00435
ACS Energy Lett. 2018, 3, 1315−1324

(49) Toberer, E. S.; Zevalkink, A.; Crisosto, N.; Snyder, G. J. The Zintl compound $Ca_5Al_2Sb_6$ for low-cost thermoelectric power generation. *Adv. Funct. Mater.* **2010**, *20*, 4375−4380.
(50) Zevalkink, A.; Toberer, E. S.; Zeier, W. G.; Flage-Larsen, E.; Snyder, G. J. Ca_3AlSb_3: an inexpensive, non-toxic thermoelectric material for waste heat recovery. *Energy Environ. Sci.* **2011**, *4*, 510−518.
(51) Zevalkink, A.; Zeier, W. G.; Pomrehn, G.; Schechtel, E.; Tremel, W.; Snyder, G. J. Thermoelectric properties of Sr_3GaSb_3 - a chain-forming Zintl compound. *Energy Environ. Sci.* **2012**, *5*, 9121−9128.
(52) Seshadri, R.; Hill, N. A. Visualizing the role of Bi 6s "lone pairs" in the off-center distortion in ferromagnetic $BiMnO_3$. *Chem. Mater.* **2001**, *13*, 2892−2899.
(53) Božin, E. S.; Malliakas, C. D.; Souvatzis, P.; Proffen, T.; Spaldin, N. A.; Kanatzidis, M. G.; Billinge, S. J. L. Entropically stabilized local dipole formation in lead chalcogenides. *Science* **2010**, *330*, 1660.
(54) Tyagi, K.; Gahtori, B.; Bathula, S.; Srivastava, A. K.; Shukla, A. K.; Auluck, S.; Dhar, A. Thermoelectric properties of Cu_3SbSe_3 with intrinsically ultralow lattice thermal conductivity. *J. Mater. Chem. A* **2014**, *2*, 15829−15835.
(55) He, Y.; Day, T.; Zhang, T.; Liu, H.; Shi, X.; Chen, L.; Snyder, G. J. High thermoelectric performance in non-toxic earth-abundant copper sulfide. *Adv. Mater.* **2014**, *26*, 3974−3978.
(56) Olvera, A. A.; Moroz, N. A.; Sahoo, P.; Ren, P.; Bailey, T. P.; Page, A. A.; Uher, C.; Poudeu, P. F. P. Partial indium solubility induces chemical stability and colossal thermoelectric figure of merit in Cu_2Se. *Energy Environ. Sci.* **2017**, *10*, 1668−1676.
(57) Guin, S. N.; Pan, J.; Bhowmik, A.; Sanyal, D.; Waghmare, U. V.; Biswas, K. Temperature dependent reversible p-n-p type conduction switching with colossal change in thermopower of semiconducting AgCuS. *J. Am. Chem. Soc.* **2014**, *136*, 12712−12720.
(58) Liu, Z.; Mao, J.; Sui, J.; Ren, Z. High thermoelectric performance of a-MgAgSb for power generation. *Energy Environ. Sci.* **2018**, *11*, 23−44.
(59) Liu, Z.; Geng, H.; Mao, J.; Shuai, J.; He, R.; Wang, C.; Cai, W.; Sui, J.; Ren, Z. Understanding and manipulating the intrinsic point defect in α-MgAgSb for higher thermoelectric performance. *J. Mater. Chem. A* **2016**, *4*, 16834−16840.

DOI: 10.1021/acsenergylett.8b00435
ACS Energy Lett. 2018, 3, 1315−1324